frontiers in Materials

ORIGINAL RESEARCH
published: 20 August 2021
doi: 10.3389/fmats.2021.748687

Hierarchical Structure Fabrication of IPMC Strain Sensor With High Sensitivity

Longfei Chang[1,2], Dongping Wang[1], Jiajia Hu[1], Yan Li[1], Yanjie Wang[3] and Ying Hu[1,2]**

[1]Anhui Province Key Lab of Aerospace Structural Parts Forming Technology and Equipment, Hefei University of Technology, Hefei, China, [2]Anhui Province Key Lab of Advanced Functional Materials and Devices, Hefei University of Technology, Hefei, China, [3]School of Mechanical and Electrical Engineering, Changzhou Campus, Hohai University, Changzhou, China

In this paper, a biological template method is introduced and investigated to fabricate ionic polymer-metal composite (IPMC) strain sensor with bionic hierarchical structures. We utilized the multi-level structure of reed leaf surface, which can improve the contact area between the substrate and the electrode layers. Hierarchical structures were observed on the IPMC samples, including pyramid strips with the width in the range of 60–80 μm as well as synaptic scatters with diameter around 10 μm. In addition, five kinds of sensors with different interface structures were obtained by combining the traditional microneedle roller roughening and chemical plating processes. It was found that the IPMC sensor with reed-leaf and microneedle structure on each side presented the best performance, along with a high linearity, a sensitivity of 62.5 mV/1% and a large generated voltage peak under given mechanical stimuli, which is 3.7 times that of the sample fabricated without roughening.

Keywords: ionic polymer-metal composite, biological template, ionic sensor, wearable sensing, roughness identification

OPEN ACCESS

Edited by:
Xufeng Dong,
Dalian University of Technology, China

Reviewed by:
Yingdan Liu,
Yanshan University, China
Zicai Zhu,
Xi'an Jiaotong University, China

****Correspondence:***
Yanjie Wang
yjwang@hhu.edu.cn
Ying Hu
huying@hfut.edu.cn

Specialty section:
This article was submitted to Smart Materials, a section of the journal Frontiers in Materials

Received: *28 July 2021*
Accepted: *09 August 2021*
Published: *20 August 2021*

Citation:
Chang L, Wang D, Hu J, Li Y, Wang Y and Hu Y (2021) Hierarchical Structure Fabrication of IPMC Strain Sensor With High Sensitivity. Front. Mater. 8:748687. doi: 10.3389/fmats.2021.748687

INTRODUCTION

Owing to the growing demand of arbitrary surface sensing in soft electro-mechanical systems, such as wearable electronic equipment and artificial intelligent devices, soft strain sensors have been explored extensively due to their inherent advantages including biocompatibility, high flexibility and sensitivity, as well as large sensing range (Amjadi et al., 2016; Gao et al., 2019; Wang et al., 2019; Dong et al., 2020; Wang et al., 2020). According to the sensing mechanism, soft strain sensors can be generally classified into piezoresistance type (Ma et al., 2018; Feng et al., 2019; Yin et al., 2019), capacitance type (Mannsfeld et al., 2010; Pang et al., 2015; Yoo et al., 2018), nanofriction type (Niu et al., 2013; Zheng et al., 2017; Huang et al., 2021), piezoelectric type (Nguyen, 2019; Stadlober et al., 2019) and ionic type (Han et al., 2017; Panwar and Gopinathan, 2019). Among them, the ionic strain sensors can generate electrical signals through the migration and redistribution of internal ions under mechanical deformation, during which no electrical source was compulsive, and a strain sensitivity with direction recognition function was presented (Liu et al., 2016).

Ionic polymer-metal composite (IPMC) is a typical ionic strain sensor with promising electro-mechanical conversion performance (Ming et al., 2018). It is usually consisting of an ionic exchange membrane sandwiched between two electrode layers. During the past few years, increasing research accentuated the importance of rough interfaces during the electro-mechanical performance of IPMC, which attracts a growing attention on its interface optimization. The contact interface between the electrode and the substrate polymer usually carried a rough characteristic of mutual penetration, which affects the mass transport path, and subsequently the charge accumulation; therefore, it plays an important role in the electrical and mechanical

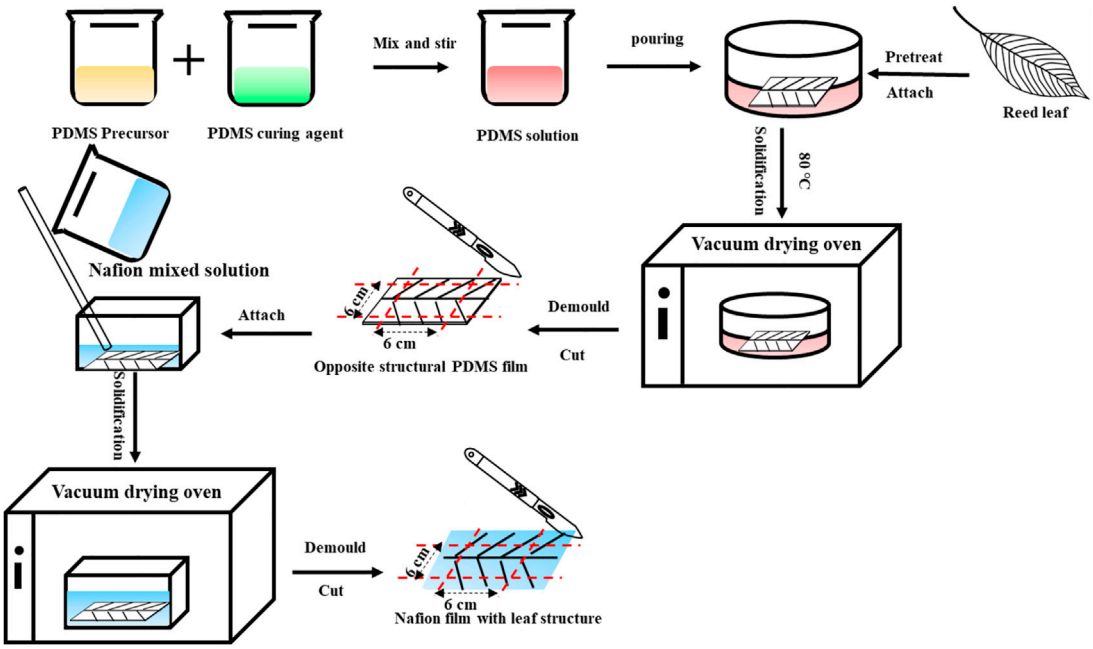

FIGURE 1 | Preparation process of the substrate membrane with biomimetic template.

transduction process. Although some roughening methods, including sandpaper grinding (Tamagawa et al., 2002; Stoimenov et al., 2006), chemical etching (Kim et al., 2007), sandblasting (Wang et al., 2016), plasma etching (Choi et al., 2008; Saher et al., 2010), mould casting Noh et al. (2002), He et al. (2013) and microneedle rolling (Chang et al., 2019) were proved effective to increase the contact interface between the electrodes and the substrate of IPMC, it still leaves much room for further probing on the property enhancement introduced by new interface manipulation (Seol et al., 2014; Sun et al., 2017; Xia et al., 2017; Shi et al., 2019; Zhao et al., 2019).

In this paper, a biological template method in combination with chemical plating was proposed to fabricate IPMC sensors with bionic hierarchical structures. The results showed that the sensitivity of a reed-leaf-structure sensor can reach up to 62.5 mV/1%. More rich and diversified structure including triangular pyramids with width of 60–80 μm as well as synapses with diameter of about 10 μm were observed on the surface of the sensors fabricated with reed-leaf template, which we believe would contribute to its ability of identifying the object surface and may interpret their outstanding performances. In addition, the application of the reed-leaf structure ionic sensor was explored in some facial expression detecting and object surface identification. Based on the experimental analysis on reed-leaf-structure IPMC sensor, this paper is expected to present an instruction for the future interface design and the performance optimization of IPMC sensors.

THE EXPERIMENTAL

Fabrication Process of IPMC Sensors

1) Preparation of Nafion film with biological surface

The biological template method is to replicate the microstructure of biological surface on the target substrate. In our experiment, polydimethylsiloxane (PDMS) solution was utilized to cast a film with contrary structure of biological surface as an intermediate process. In addition, the surface structure of PDMS membrane was duplicated by solution casting method, and Nafion membrane with the same structure as the leaf was obtained, as illustrated in **Figure 1**. The specific preparation process is as follows.

Preparation of PDMS film with the contrary structure: firstly, a naturally-dried reed leaf was cleaned with deionized (DI) water, cut to appropriate size, and boiled in DI bath (100°C, 4 h). Take out the leaf, arrange it evenly on the filter paper and press them (0.1 MPa, 80°C, 48 h). Attach the dry and flat leaf to the bottom of the glass mold with double-sided adhesive tape. At the same time, PDMS precursor and curing agent with a ratio of 10:1 were stirred for 30 min and vacuum treated for 20 min. Then, pour the mixed PDMS solution into the glass mold for curing (80°C, 4 h). Afterwards, separate the PDMS film with contrary structure from the reed leaf, cut it into a size of 6 × 6 cm and attach it to the bottom of the glass mold for next process.

Preparation of Nafion film with the same structure as the leaf: To prepare a bionic Nafion film with thickness of 150 μm and area of 6 × 6 cm, around 23 g Nafion (5%) solution and 8 g N, N-Dimethylacetamide (DMAC) solution were needed and processed with heating, mixing and stirring (50°C, 500 r/ min, 6 h). Pour the mixed solution into the glass mold with PDMS template and vacuum it until no macroscopic bubbles can be observed in the mixture. Finally, curing treatment (90°C, 24 h) and heat treatment (120°C, 30 min) were carried out.

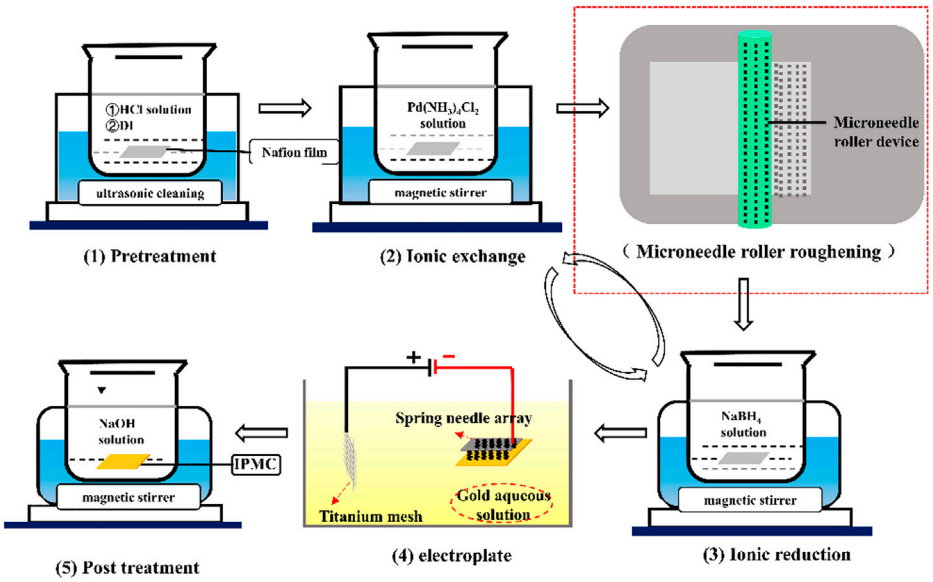

FIGURE 2 | Preparation process of IPMC.

2) Fabrication of IPMC

IPMC samples with Palladium (Pd) and gold (Au) electrodes were fabricated to evaluate the influence of biological structure on the sensing properties of ionic sensor. The fabrication process typically consists of 5 steps: pretreatment, impregnation-reduction plating (IRP), electroplating (EP) and post-treatment, as shown in **Figure 2**.

Pretreatment: Nafion film was treated successively in ultrasonic water bath (100 Hz, 30 min), hydrochloric acid (2 mol/ L, 100°C, 30 min) and DI water (100°C, 30 min) for purification.

IRP: Immerse the pretreated substrate film in $Pd(NH_3)_4Cl_2$ solution (0.01 mol/ L) for ionic exchange with magnetic stirring (250 r/ min, 50°C, 2 h). Then, reduce the Pd complex cations in the membrane with NaBH4 alkaline solution (0.01 mol/ L, pH > 13), along with heating and stirring (50 r/ min, 50°C). Add 3 ml of the NaBH4 solution (1.37 mol/ L) every 30 min to enhance the reduction process. The above process was repeated twice.

EP: Cut the edge of Pd-IPMC to prevent the short circuit of electrodes on both sides and immerse the sample in the gold plating electrolyte with a concentration of 1.2 g/ L. Contact the cathode spring needle with the target surface, and the anode with a titanium mesh, under a voltage of 5 V and current of 0.1 A. The plating time for one surface of our samples was 10 min.

Post-treatment: Immerse the Au-Pd-IPMC after electroplating in NaOH solution, along with mild heating and stirring (0.2 mol/ L, 250 r/ min, 50°C, 2 h).

For comparison, we also prepared the unstructured interface and microneedle rolling interface, which was fabricated according to our formerly proposed roughening method (600 times rolling, needle length: 2.5 mm, needle diameter: 0.2 mm, load: 1,000 g) (Chang et al., 2019). The membrane was roughened after the first impregnation process. According to our exploratory experiments, when roughening before the ion exchange, the pores or rough grooves in the membrane will be squeezed together by the shrinking during ion exchange, which is not conducive to the formation of needle-like penetrating interface electrodes. The roller used for the fabrication in this paper was with a length of 35 mm, needle diameter of 20 mm and exposed needle height of 2.5 mm. Between the ionic exchange and ionic reduction steps, the films were rinsed with DI water and then fixed to a clean base glass by tape on the edge. The roller loaded with a mass of 1000 g was horizontally pushed uniformly back and forth on the surface for total 600 circles, with the film being rotated by 90° after roughening of every 150 cycles. The fabrication of IPMC with microneedle roller roughening is illustrated as in the red dotted block in **Figure 2**. All the samples were fabricated with the same plating process.

TABLE 1 | Process combination of the IPMC sensor samples.

Marking	Different fabrication combination
LN	Reed leaf template/Non-roughening
LR	Reed leaf template/Microneedle roller roughening
RN	Microneedle roller roughening/Non-roughening
RR	Both sides with microneedle roller roughening
NN	Both sides without roughening

IPMC Sample Design

In order to compare the influences of interface structure on the sensing performance, five samples with different interface structures were prepared, as listed in **Table 1**. The substrate surface roughened with microneedle roller is marked as R; the surface without roughening is marked as N and that fabricate with the reed leaf template is marked as L. Among these samples, the LN and LR were fabricated based on the Nafion film fabricated with the reed leaf template, while the others were with the casting Nafion film

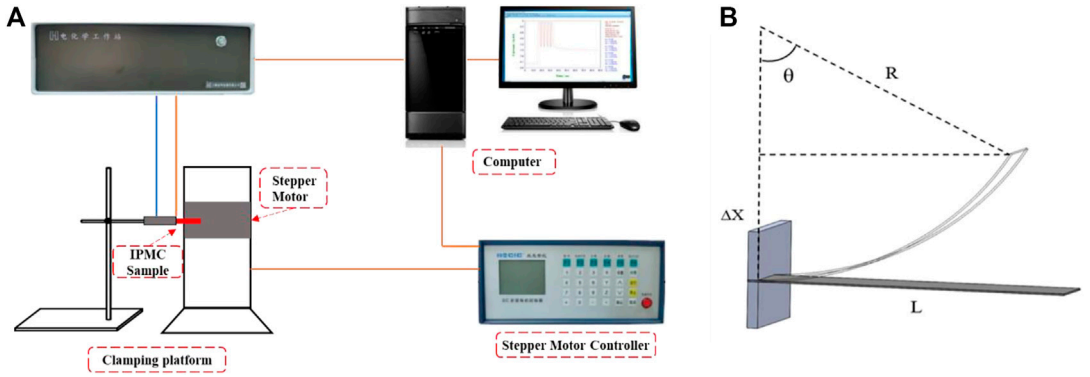

FIGURE 3 | The test platform of IPMC sensor. **(A)** The setup for sensing performance measuring. **(B)** The schematic diagram of the cantilever configuration.

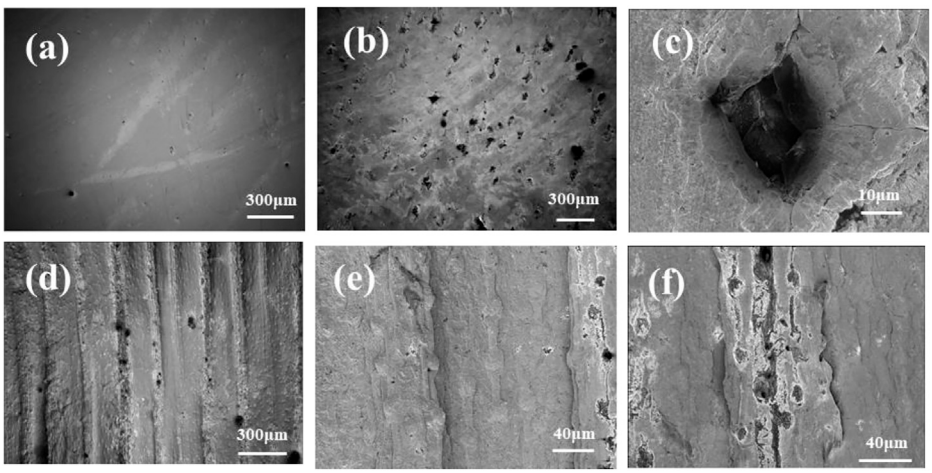

FIGURE 4 | The surface SEM images of IPMC films with different microstructures. **(A)** Surface of sample NN. **(B-C)** Surface structure of sample RR. **(D-F)** The surface biological structure in sample LN.

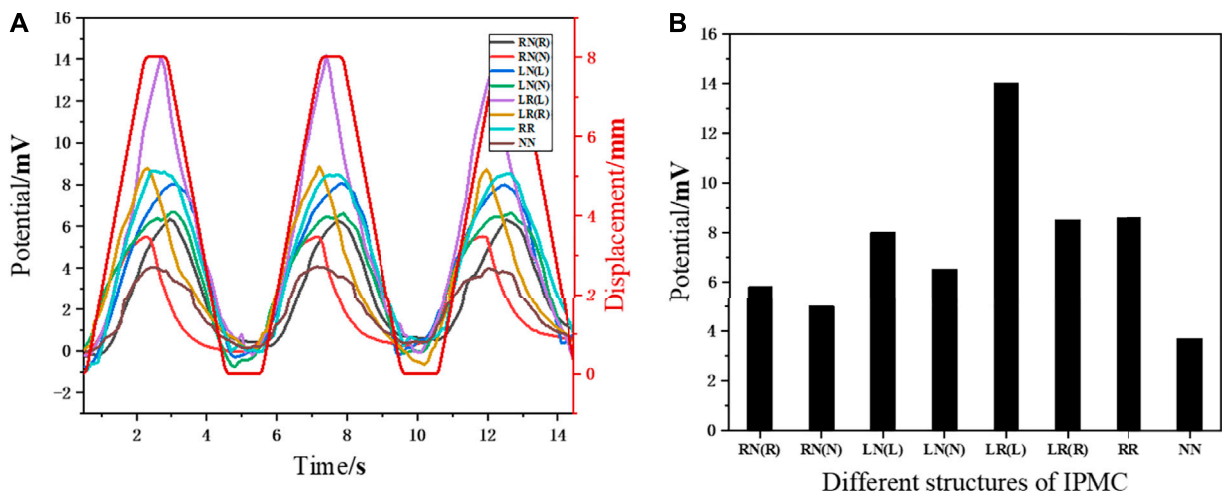

FIGURE 5 | Voltage generated by the five IPMC samples. **(A)** The instantaneous real-time response of IPMC samples with the comparison of the displacement stimuli. **(B)** The diagram of the generated peak voltage value.

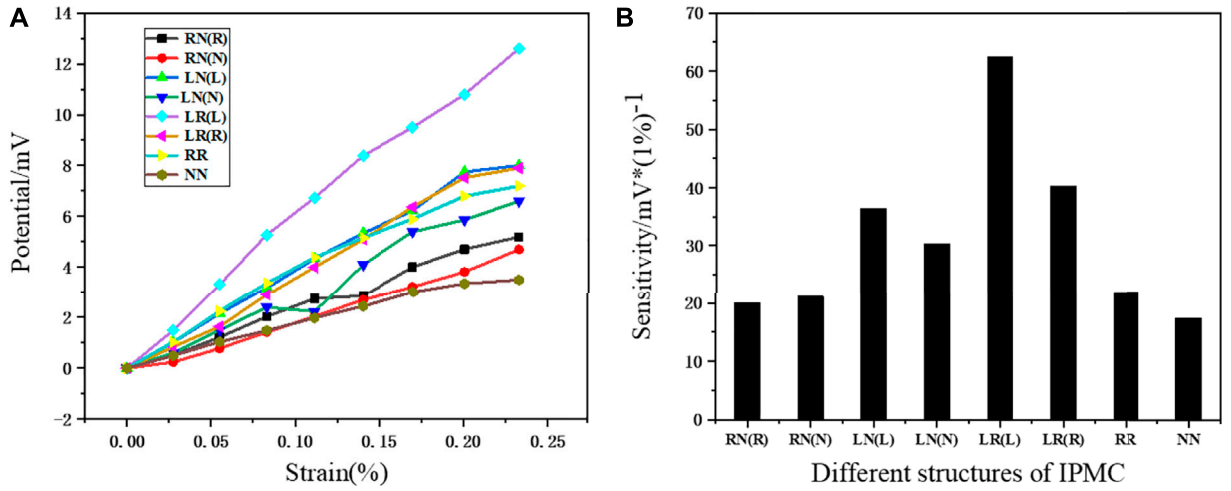

FIGURE 6 | The linearity and sensitivity of the IPMC samples. **(A)** The strain-voltage curve. **(B)** The gauge factor value comparison diagram.

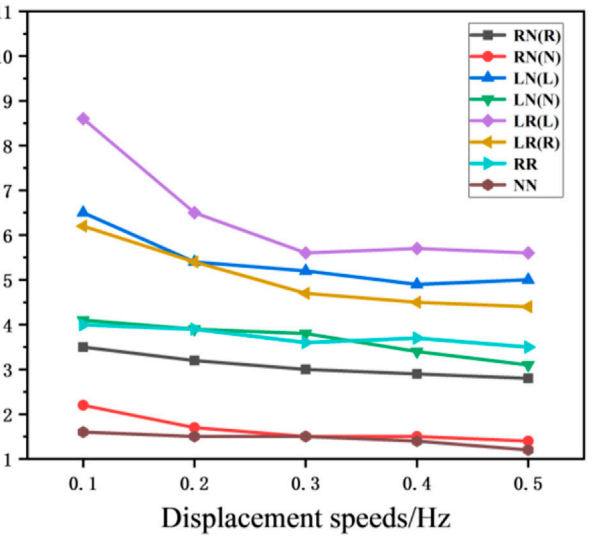

FIGURE 7 | The sensing voltage of the IPMC samples under displacement speed.

fabricated with flat glass mold. Taking LR for example, the non-templating side of the substrate was treated with micro roller roughening, followed by the above-mentioned plating process.

Measurement Platform and Methods

The sensing performance of IPMC was tested with a specific platform, with the sample fixed in a cantilever configuration, as illustrated in **Figure 3**. The test platform mainly consisted with a displacement generation system controlled by a stepper motor controller and a voltage signal acquisition system regulated by an electrochemical work station. During operation, the parameters of the stepper motor controller were set, including relative motion distance (8 mm for our experiments), cyclic times and speed frequency. Then, the front clamp of the stepper motor was contacted with the end point of the IPMC sample, and a forward and backward reciprocating movement of the front clamp was used to drive the IPMC sample fixed on the clamping platform to produce a bending deformation, thus generating the sensing voltage signal, which was collected and processed by the electrochemical workstation.

As can be seen from **Figure 3B**, the bending strain of IPMC film can be calculated based on the cantilever geometry. Before measurement, the film was placed in a flat state. The strain ε corresponding to the bending deformation ΔX can be obtained with **Eq. 1**, according to the classic beam theory.

$$\varepsilon = h/2R \tag{1}$$

Where h is thickness of the film, which is 0.11 mm for our samples, R is the curvature. And R can be derived from the following formulas.

$$\theta \cdot R = L \tag{2}$$

$$R(1 - cos\theta) = \Delta X \tag{3}$$

Where L is the length of IPMC film, which is 2 cm, θ is the central angle.

The sensitivity of the sensor, evaluated by the gauge factor GF, is calculated by the relationship between generated voltage V and strain, as in **Equation 4**.

$$GF = (V - V_0)/\varepsilon \tag{4}$$

Where V_0 is the initial voltage when the IPMC is in free state.

RESULTS AND DISCUSSION

Microscopic Morphology

In order to distinguish the surface structure characteristics, the Nafion films processed after the first IRP were observed with

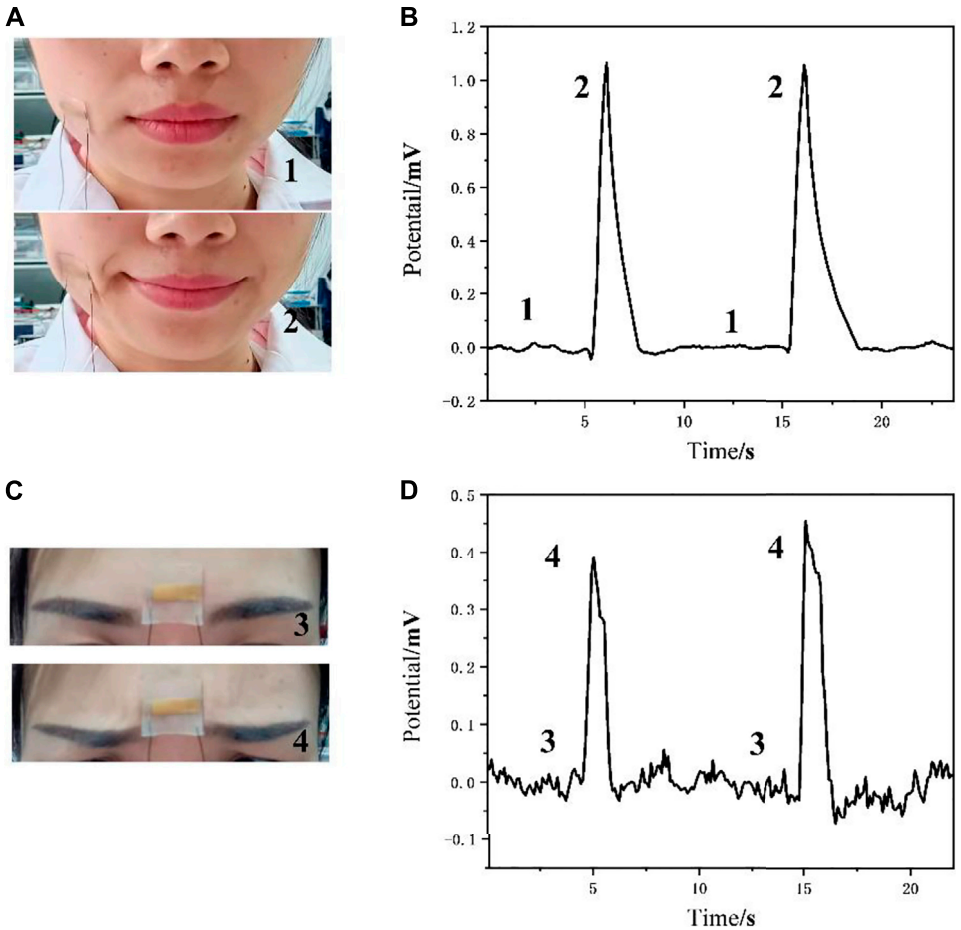

FIGURE 8 | Facial expression recognition. **(A)** Image of the IPMC sensor taped on the muscle around the mouth, 1 refers to the state without smiling; 2 is the state when smiling. **(B)** Voltage response of face muscle shifting from being expressionless to smile. **(C)** Image of the IPMC sensor taped on the eyebrow center; 3 means no frowning; 4 means frowning. **(D)** Voltage response during frowning.

scanning electron microscopy (SEM). The **Figure 4A** shows the surface without roughening. The surface is smooth and small holes can be found occasionally, which might be ascribed to the expansion and contraction process during the plating. **Figures 4B,C** are the SEM pictures of the surface fabricated with the microneedle roller roughening. The surfaces are covered with holes of uneven size, with the diameters in the range of 20–100 μm. **Figures 4D–F** is the SEM image of the surfaces fabricated with reed leaf template. Many triangular pyramid structures can be found, of which the entire stripe is not completely vertical to the section and the width is in the range of 60–80 μm. Some round synapses were scattered on the bottom of the vertebral body, with a diameter around 10 μm. This hierarchical structure may contribute to the accumulation of the sensing charge and the increasing sensitivity to the contact surface characteristics.

Sensing Performance

To investigate the influences of interface structures on the sensing performances, the generated voltage of the 5 samples with the application of mechanical displacement was recorded, as illustrated in **Figure 5**. Some of the samples with asymmetric electrodes would present different sensing properties when bending in opposite direction. For example, LR (L) means the sample LR bending towards the leaf template (L) surface direction. The instantaneous voltage and displacement curve were compared, with a route of 8 mm and velocity of 0.3 Hz. The sensing voltage of all the IPMC samples has strong periodicity and is positively correlated with the displacement. The **Figure 5B** showed the maximum voltage produced by different structural sensors at the peak displacement point. It can be seen that all the 4 samples with microstructure interface, both microneedle interface and reed leaf template, displayed higher voltage compared to that with flat interface, indicating a distinct promoting effect of the interface structure on the mass transporting and subsequently the voltage generation. The peak voltage of sample RR was 8.6 mV, which was 2.3 times that of NN (3.7 mV), while the peak voltage of sample LR (L) and LR (R) were 14 and 8.6 mV, which are 3.7 times and 2.3 times that of NN, respectively. The distinct voltage increased from sample NN to sample LN and from RN to LR provided sound evidence for the performance improvement resulted from the hierarchical structure of the leaf template.

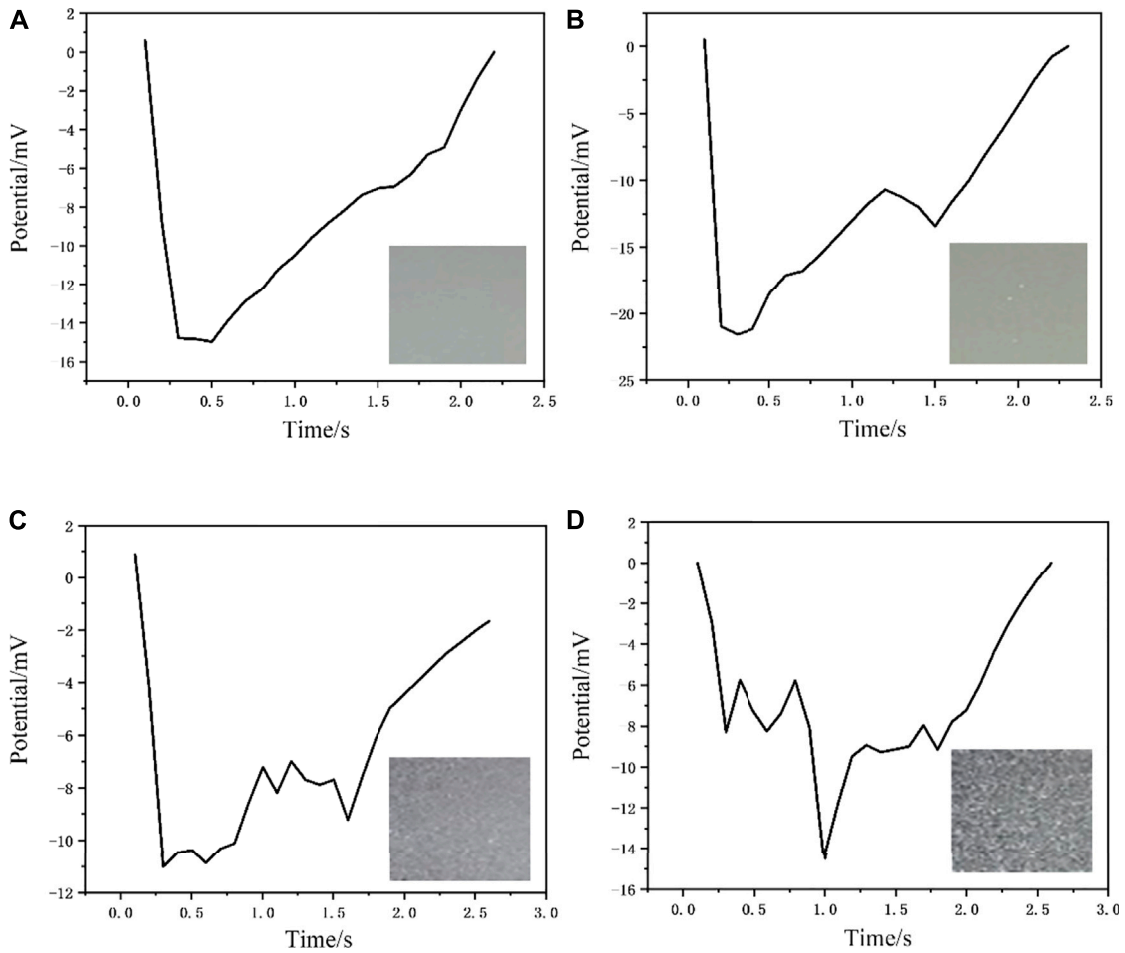

FIGURE 9 | Voltage response of sensor sliding upon surface of different roughness. **(A)** Smooth A4 paper; **(B)** Sandpaper of 800 #; **(C)** Sandpaper of about 600 #; **(D)** Sandpaper of about 320 #.

To evaluate the linearity and sensitivity of these IPMC sensors, the strain and the gauge factor were calculated based on the above-mentioned equations, as displayed in **Figure 6**. It can be found that all the IPMC samples exhibited a good linearity during the corresponding range, especially the sample LR when bending towards the leaf structure direction. In addition, the gauge factor for test LR(L) was as high as 62.5 mV/1%, indicating the highest sensitivity among these samples. For comparison, the sensitivity of the sensor NN is 17.6 mV/1%, approximately 28.1% of that for LR(L) and 80.3% of that for RR. It can be deduced that the rich micro structure might contribute to the increasing linearity and sensitivity.

The voltage response under different displacement speeds was displayed in **Figure 7**. The voltage amplitudes of all the samples had a downward trend with the increase of displacement velocity, which was a distinct characteristic of ionic transport. This trend is especially dominating for sample LR and LN. The hierarchical structure induced by the biological template increased the length as well as the complexity of the path for mass transport, subsequently enhanced the frequency-dependency of the sensors.

APPLICATION EXPLORING

Flexible sensors were widely explored in intelligent wearable devices. Combined with the characteristics of bionic structure flexible sensor, such as good adhesion to skin, biocompatibility and high sensitivity, some application exploration in expression recognition and roughness recognition were carried out to display the unique properties of those fabricated IPMC sensors. Two electrode sides of the sensors were connected with the conductive wire by using silver glue, and the voltage signals were recorded by electrochemical workstation.

Expression Recognition

In recent years, with the development of human computer interaction and wearable devices, movement sensing including expression recognition attracted growing attention. People's expressions are diversified and closed related to the mild movement of facial muscles. Here two of the IPMC strips fabricated with biological template were taped with VHB (Very High Bond, Acrylic foam tape, 3 M™) adhesive around the corner of an experimenter's mouth and the center of her eyebrows, respectively, to detect facial expressions. As shown in **Figure 8**,

when the experimenter shifted from being expressionless to a smile expression, the corners of her mouth raised, and the corresponding sensor strip generated an identifiable pulse voltage signal, while if the experimenter shifted to a frowning expression, the upper sensor wound gave a voltage peak. The voltage pulses were observed immediately with the expression change, well indicating the feasibility of IPMC sensor utilizing in facial expression detecting.

Roughness Identification

Haptic feedback is an important sensing technique, which is of great potential in the design of soft electro-mechanical devices. The sensing of textures or other surface properties provides possibility for adaptable lifting and flexible contact, which are unique instinct for almost every living being yet quite difficult to realize with traditional mechanical designs.

Inspired by the fingerprint microstructure to touch and pick up objects, IPMC with hierarchical interface were probed in roughness recognition. A IPMC strip of above-mentioned sample LR was taped to the index fingertip with VHB, with the reed leaf structure surface contacting the object surface. Sliding the fingertip sensor on object surfaces with increasing roughness, successively a A4 paper, sandpaper of about 800 Grit (800 #), 600# and 320#, and the generated voltage were recorded as illustrated in **Figure 9**. When sliding upon a smooth A4 paper, the sensor displayed a single voltage pulse; while upon the rough sandpapers, more disordered peaks appeared. Putting aside the amplitude difference mainly resulted from the pressure variation, it can be seen that, with the increase of surface roughness, the noise peaks of the voltage increased visibly. The microcosmic contact and departure of the object surface with the two-scaled structure, the triangular pyramid strip and the synapses, induced several local stress pulses and subsequently led to multiple voltage peaks. We believe this IPMC sensor can be incorporated into wearable medical equipment to achieve artificial tactile sensation for human-computer interaction devices with further manipulation design.

CONCLUSION

In this paper, we proposed a biological template method to fabricate IPMC strain sensors with bionic hierarchical structure. Reed leaf was chosen as the template due to its rich microstructure, and with PDMS utilized as an intermediate template material, the bionic structure was copied to the surface of the IPMC substrate membrane successfully. The two-scaled rough interface, including triangular strips and synaptic structures, contributed to the sensing performance of IPMC sensors. By comparing five groups of different structural samples, it is found that reed leaf/microneedle roughened sensor can achieve the highest sensitivity of 62.5 mV/1%, along with high linearity. In addition, facial expression recognition and rough surface identification were explored primarily with the new IPMC sensor. We hope this new fabrication method can inspire more strategy on the performance improvement of ionic sensors and promote future exploration on their diversified application.

DATA AVAILABILITY STATEMENT

The raw data supporting the conclusions of this article will be made available by the authors, without undue reservation.

AUTHOR CONTRIBUTIONS

LC, YW, and YH contributed to the proposing of the conception in this study and the modification of the paper's layout LC wrote the manuscript YW and YH helped to perform the analysis with constructive discussions DW and JH performed the experiments and contributed significantly to the analysis and manuscript preparation YL contributed to the plotting of diagrams and corresponding illustrations.

FUNDING

The authors acknowledge the financial support from the Natural Science Foundation of China (No.52075140), the Fundamental Research Funds for the Central Universities of China (No.PA2020GDSK0074, JZ2020HGTB0013), and the Anhui Provincial Natural Science Foundation (2008085J22).

REFERENCES

Amjadi, M., Kyung, K.-U., Park, I., and Sitti, M. (2016). Stretchable, Skin-Mountable, and Wearable Strain Sensors and Their Potential Applications: A Review. *Adv. Funct. Mater.* 26, 1678–1698. doi:10.1002/adfm.201504755

Chang, L., Yang, Q., Niu, Q., Wang, Y., Liu, Y., Lu, P., et al. (2019). High-performance Ionic Polymer-Metal Composite Actuators Fabricated with Microneedle Roughening. *Smart Mater. Struct.* 28, 015007. doi:10.1088/1361-665x/aaee26

Choi, N.-J., Lee, H.-K., Jung, S., Lee, S., and Park, K.-H. (2008). Electroactive Polymer Actuator with High Response Speed through Anisotropic Surface Roughening by Plasma Etching. *J. Nanosci. Nanotechnol.* 8, 5385–5388. doi:10.1166/jnn.2008.1433

Dong, K., Peng, X., and Wang, Z. L. (2020). Fiber/Fabric-Based Piezoelectric and Triboelectric Nanogenerators for Flexible/Stretchable and Wearable Electronics and Artificial Intelligence. *Adv. Mater.* 32, 1902549. doi:10.1002/adma.201902549

Feng, P., Ji, H., Zhang, L., Luo, X., Leng, X., He, P., et al. (2019). Highly Stretchable Patternable Conductive Circuits and Wearable Strain Sensors Based on Polydimethylsiloxane and Silver Nanoparticles. *Nanotechnology* 30, 185501. doi:10.1088/1361-6528/ab013b

Gao, W., Ota, H., Kiriya, D., Takei, K., and Javey, A. (2019). Flexible Electronics toward Wearable Sensing. *Acc. Chem. Res.* 52, 523–533. doi:10.1021/acs.accounts.8b00500

Han, S., Zhao, J., Wang, D., Lu, C., and Chen, W. (2017). Bionic Ion Channel and Single-Ion Conductor Design for Artificial Skin Sensors. *J. Mater. Chem. B* 5, 7126–7132. doi:10.1039/C7TB01760J

He, Q., Yu, M., Zhang, X., and Dai, Z. (2013). Electromechanical Performance of an Ionic Polymer-Metal Composite Actuator with Hierarchical Surface Texture. *Smart Mater. Struct.* 22, 055001. doi:10.1088/0964-1726/22/5/055001

Huang, P., Wen, D.-L., Qiu, Y., Yang, M.-H., Tu, C., Zhong, H.-S., et al. (2021). Textile-Based Triboelectric Nanogenerators for Wearable Self-Powered Microsystems. *Micromachines* 12, 158. doi:10.3390/mi12020158

Kim, S. J., Lee, I. T., and Kim, Y. H. (2007). Performance Enhancement of IPMC Actuator by Plasma Surface Treatment. *Smart Mater. Struct.* 16, N6–N11. doi:10.1088/0964-1726/16/1/n02

Liu, Y., Hu, Y., Zhao, J., Wu, G., Tao, X., and Chen, W. (2016). Self-Powered Piezoionic Strain Sensor toward the Monitoring of Human Activities. *Small* 12, 5074–5080. doi:10.1002/smll.201600553

Ma, Z., Wei, A., Ma, J., Shao, L., Jiang, H., Dong, D., et al. (2018). Lightweight, Compressible and Electrically Conductive Polyurethane Sponges Coated with Synergistic Multiwalled Carbon Nanotubes and Graphene for Piezoresistive Sensors. *Nanoscale* 10, 7116–7126. doi:10.1039/c8nr00004b

Mannsfeld, S. C. B., Tee, B. C.-K., Stoltenberg, R. M., Chen, C. V. H.-H., Barman, S., Muir, B. V. O., et al. (2010). Highly Sensitive Flexible Pressure Sensors with Microstructured Rubber Dielectric Layers. *Nat. Mater* 2010 9, 859–864. doi:10.1038/nmat2834

Ming, Y., Yang, Y., Fu, R. P., Lu, C., Zhao, L., Hu, Y. M., et al. (2018). IPMC Sensor Integrated Smart Glove for Pulse Diagnosis, Braille Recognition, and Human-Computer Interaction. *Adv. Mater. Technol.* 3, 1800257. doi:10.1002/admt.201800257

Nguyen, D.-N. W. (2019). Fabrication and Characterization of a Flexible PVDF Fiber-Based Polymer Composite for High-Performance Energy Harvesting Devices. *J. Sens. Sci. Technol.* 28, 205–215. doi:10.5369/jsst.2019.28.4.205

Niu, S., Liu, Y., Wang, S., Lin, L., Zhou, Y. S., Hu, Y., et al. (2013). Theory of Sliding-Mode Triboelectric Nanogenerators. *Adv. Mater.* 25, 6184–6193. doi:10.1002/ADMA.201302808

Noh, T.-G., Tak, Y., Nam, J.-D., and Choi, H. (2002). Electrochemical Characterization of Polymer Actuator with Large Interfacial Area. *Electrochimica Acta* 47, 2341–2346. doi:10.1016/s0013-4686(02)00089-0

Pang, C., Koo, J. H., Nguyen, A., Caves, J. M., Kim, M.-G., Chortos, A., et al. (2015). Highly Skin-Conformal Microhairy Sensor for Pulse Signal Amplification. *Adv. Mater.* 27, 634–640. doi:10.1002/adma.201403807

Panwar, V., and Gopinathan, A. (2019). An Ionic Polymer-Metal Nanocomposite Sensor Using the Direct Attachment of an Acidic Ionic Liquid in a Polymer Blend. *J. Mater. Chem. C* 7, 9389–9397. doi:10.1039/c9tc02355k

Saher, S., Kim, W., Moon, S., Jin Kim, H., and Kim, Y. H. (2010). Electro-actuation Characteristics of Cl2and SF6plasma-Treated IPMC Actuators. *Smart Mater. Struct.* 19, 105013. doi:10.1088/0964-1726/19/10/105013

Seol, M.-L., Woo, J.-H., Lee, D.-I., Im, H., Hur, J., and Choi, Y.-K. (2014). Nature-Replicated Nano-In-Micro Structures for Triboelectric Energy Harvesting. *Small* 10, 3887–3894. doi:10.1002/smll.201400863

Shi, J., Lv, S., Wang, L., Dai, Z., Yang, S., Zhao, L., et al. (2019). Crack Control in Biotemplated Gold Films for Wide-Range, Highly Sensitive Strain Sensing. *Adv. Mater. Inter.* 6, 1901223. doi:10.1002/admi.201901223

Stadlober, B., Zirkl, M., and Irimia-Vladu, M. (2019). Route towards Sustainable Smart Sensors: Ferroelectric Polyvinylidene Fluoride-Based Materials and Their Integration in Flexible Electronics. *Chem. Soc. Rev.* 48, 1787–1825. doi:10.1039/c8cs00928g

Stoimenov, B. L., Rossiter, J. M., and Mukai, T. (2006). Anisotropic Surface Roughness Enhances the Bending Response of Ionic Polymer-Metal Composite (IPMC) Artificial Muscles. *Smart Mater. IV* 6413, 641302. doi:10.1117/12.695665

Sun, J.-G., Yang, T. N., Kuo, I.-S., Wu, J.-M., Wang, C.-Y., and Chen, L.-J. (2017). A Leaf-Molded Transparent Triboelectric Nanogenerator for Smart Multifunctional Applications. *Nano Energy* 32, 180–186. doi:10.1016/j.nanoen.2016.12.032

Tamagawa, H., Yagasaki, K., and Nogata, F. (2002). Mechanical Characteristics of Ionic Polymer-Metal Composite in the Process of Self-Bending. *J. Appl. Phys.* 92, 7614–7618. doi:10.1063/1.1516269

Wang, C., Xia, K., Wang, H., Liang, X., Yin, Z., and Zhang, Y. (2019). Advanced Carbon for Flexible and Wearable Electronics. *Adv. Mater.* 31, 1801072. doi:10.1002/adma.201801072

Wang, Y., Liu, J., and Chen, H. (2016). Enhanced Electromechanical Response of Ionic Polymer-Metal Composite (IPMC) Actuators by Various Nafion Roughening Levels. *Electroact. Polym. Actuators Devices 2016* 9798, 97982X. doi:10.1117/12.2218857

Wang, Z., Cong, Y., and Fu, J. (2020). Stretchable and Tough Conductive Hydrogels for Flexible Pressure and Strain Sensors. *J. Mater. Chem. B* 8, 3437–3459. doi:10.1039/c9tb02570g

Xia, K., Wang, C., Jian, M., Wang, Q., and Zhang, Y. (2017). CVD Growth of Fingerprint-like Patterned 3D Graphene Film for an Ultrasensitive Pressure Sensor. *Nano Res. 2018* 11 (11), 1124–1134. doi:10.1007/s12274-017-1731-z

Yin, F., Li, X., Peng, H., Li, F., Yang, K., and Yuan, W. (2019). A Highly Sensitive, Multifunctional, and Wearable Mechanical Sensor Based on RGO/synergetic Fiber Bundles for Monitoring Human Actions and Physiological Signals. *Sensors Actuators B: Chem.* 285, 179–185. doi:10.1016/j.snb.2019.01.063

Yoo, J.-Y., Seo, M.-H., Lee, J.-S., Choi, K.-W., Jo, M.-S., and Yoon, J.-B. (2018). Industrial Grade, Bending-Insensitive, Transparent Nanoforce Touch Sensor via Enhanced Percolation Effect in a Hierarchical Nanocomposite Film. *Adv. Funct. Mater.* 28, 1804721. doi:10.1002/adfm.201804721

Zhao, T., Li, T., Chen, L., Yuan, L., Li, X., and Zhang, J. (2019). Highly Sensitive Flexible Piezoresistive Pressure Sensor Developed Using Biomimetically Textured Porous Materials. *ACS Appl. Mater. Inter.* 11, 29466–29473. doi:10.1021/acsami.9b09265

Zheng, Q., Shi, B., Li, Z., and Wang, Z. L. (2017). Recent Progress on Piezoelectric and Triboelectric Energy Harvesters in Biomedical Systems. *Adv. Sci.* 4, 1700029. doi:10.1002/advs.201700029

Conflict of Interest: The authors declare that the research was conducted in the absence of any commercial or financial relationships that could be construed as a potential conflict of interest.

Publisher's Note: All claims expressed in this article are solely those of the authors and do not necessarily represent those of their affiliated organizations, or those of the publisher, the editors and the reviewers. Any product that may be evaluated in this article, or claim that may be made by its manufacturer, is not guaranteed or endorsed by the publisher.